

Chirality-driven ferroelectricity in LiCuVO₄

Alexander Ruff, Peter Lunkenheimer, Hans-Albrecht Krug von Nidda, Sebastian Widmann, Andrey Prokofiev, Leonid Svistov, Alois Loidl, Stephan Krohns

Angaben zur Veröffentlichung / Publication details:

Ruff, Alexander, Peter Lunkenheimer, Hans-Albrecht Krug von Nidda, Sebastian Widmann, Andrey Prokofiev, Leonid Svistov, Alois Loidl, and Stephan Krohns. 2019. "Chirality-driven ferroelectricity in LiCuVO₄." *npj Quantum Materials* 4 (1): 24.
<https://doi.org/10.1038/s41535-019-0163-2>.

ARTICLE OPEN

Chirality-driven ferroelectricity in LiCuVO_4

Alexander Ruff¹, Peter Lunkenheimer¹, Hans-Albrecht Krug von Nidda¹, Sebastian Widmann¹, Andrey Prokofiev², Leonid Svistov³, Alois Loidl¹ and Stephan Krohns¹

Chirality or the handedness of objects is of prime importance in life science, biology, chemistry, and physics. It is also a major symmetry ingredient in frustrated magnets revealing spin-spiral ground states. Vector-chiral phases, with the twist (either clock- or counter clock-wise) between neighboring spins being ordered, but with disorder with respect to the angles between adjacent spins, have been predicted almost five decades ago. Experimental proofs, however, are rare and controversial. Here, we provide experimental evidence for such a phase in LiCuVO_4 , a one-dimensional quantum magnet with competing ferromagnetic and antiferromagnetic interactions. The vector-chiral state is identified via a finite ferroelectric polarization arising at temperatures well above the multiferroic phase exhibiting long-range three-dimensional spin-spiral and polar order. On increasing temperatures, spin order becomes suppressed at T_N , whereas chiral long-range order still exist, leaving a temperature window with chirality-driven ferroelectricity in the presence of an external magnetic field.

npj Quantum Materials (2019)4:24; <https://doi.org/10.1038/s41535-019-0163-2>

INTRODUCTION

In recent years, magnetic materials exhibiting spin spirals gained considerable attention owing to their helical or cycloidal spin configurations.¹ There the chiral spin twist can induce spin-driven ferroelectricity² either via a spin-current mechanism³ or via an inverse Dzyaloshinskii–Moriya interaction.^{4,5} This revitalized the large field of multiferroics,⁶ being of great fundamental and technological importance.^{7,8} Vector chirality, defined by the vector product of spins at adjacent lattice sites, $\mathbf{S}_i \times \mathbf{S}_j$, is one of the key concepts in quantum magnetism^{9–11} and in one-dimensional (1D) spin systems. Chirality is also an important symmetry element of spin spirals. However, either finite temperatures or quantum fluctuations can completely suppress the long-range spin order of a spiral, while leaving the chiral twist less affected, leading to a vector-chiral (VC) phase. For 1D XY helimagnets, 40 years ago Villain¹² predicted such a phase appearing between the paramagnetic (PM) high-temperature state and the conventional long-range-ordered 3D helical spin solid.

The occurrence of a VC phase results from an exponential divergence of the chirality–chirality correlation with decreasing temperature (caused by the Ising character of the chirality order parameter), whereas the spin–spin correlation diverges via a power law. Based on similar arguments, Onoda and Nagaosa¹³ proposed to search for chiral spin pairing just above the helical magnetic ordering temperature in 1D multiferroic quantum magnets. The (H, T) phase diagrams of $S = \frac{1}{2}$ magnetic chains with competing interactions are complex. A variety of phases, including spin-density wave, vector-chiral, nematic, and other multipolar phases has been theoretically elucidated.^{14–23} However, experimental explorations of these phases are rare. A possible validation of Villain’s conjecture of a VC phase was reported, based on the two-step magnetic ordering observed in the quasi-1D helimagnet $\text{Gd}(\text{hfac})_3\text{NITeT}$.²⁴ In light of the mentioned ferroelectric (FE) polarization induced by chiral spin twists,^{3–5,22} the

most promising route seems to search for VC phases by identifying FE polarization at temperatures slightly above well-known 3D-ordered spin-driven multiferroic phases.^{13,25} From a theoretical point of view, quantum spin-chain systems with ferromagnetic (FM) nearest neighbor (nn) and antiferromagnetic (AFM) next-nearest neighbor (nnn) exchange, for which the inverse spinel compound LiCuVO_4 is a prime example, seem perfectly appropriate to detect the VC phase.¹³

RESULTS

LiCuVO_4 offers a rich variety of complex magnetic phases, like the possible appearance of a bond-nematic phase at low temperatures and high magnetic fields.^{26–30} In this system, the Cu^{2+} ions carry a spin $S = \frac{1}{2}$ and form a quasi-1D Heisenberg chain with competing nn FM exchange, $J_1/k_B \approx -19\text{ K}$ and nnn AFM exchange $J_2/k_B \approx 65\text{ K}$.³¹ However, strongly varying exchange constants are reported.^{32,33} Owing to weak inter-chain coupling, this frustrated 1D spin system undergoes 3D helical order at $T_N \approx 2.5\text{ K}$,^{34,35} developing spin-driven ferroelectricity and, thus, multiferroicity.^{36,37} Here, we report the occurrence of finite FE polarization in the PM phase of LiCuVO_4 , just above the onset of 3D spin order. This FE phase, detected at moderate external magnetic fields, extends to temperatures up to five times T_N . Overall, our findings strongly point to the existence of a VC phase in the $S = \frac{1}{2}$ quantum magnet LiCuVO_4 , in accord with theoretical predictions.^{13,22}

Figure 1 shows results of heat capacity and magnetic experiments on LiCuVO_4 at low temperatures and moderate external magnetic fields (Supplementary Information, Figure S1 shows results of heat-capacity measurements up to ambient temperatures). The inset of Fig. 1a displays the temperature dependence of the magnetic susceptibility. The broad maximum is a fingerprint³⁸ of a $S = \frac{1}{2}$ linear-chain compound with an

¹Experimental Physics V, Center for Electronic Correlations and Magnetism, University of Augsburg, 86135 Augsburg, Germany; ²Institute of Solid State Physics, Vienna University of Technology, A-1040 Wien, Austria and ³P.L. Kapitza Institute for Physical Problems, RAS, Moscow 119334, Russia
Correspondence: Stephan Krohns (Stephan.krohns@physik.uni-augsburg.de)

Received: 10 January 2019 Accepted: 9 May 2019

Published online: 24 May 2019

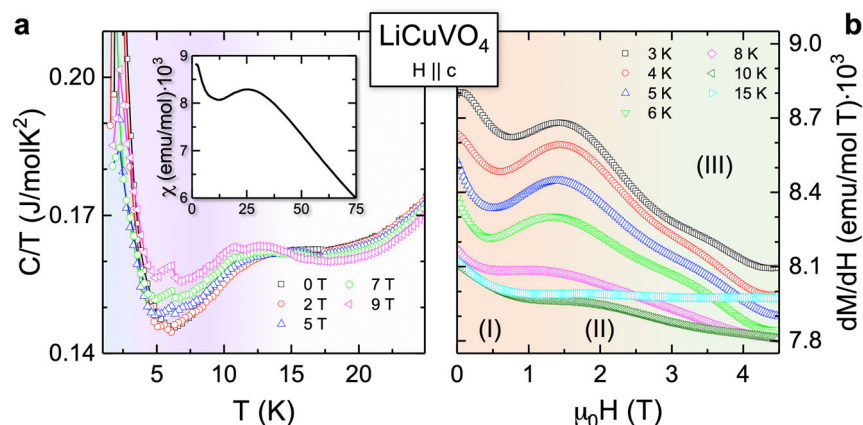


Fig. 1 Heat capacity and magnetization of LiCuVO_4 . **a** Temperature dependence of the specific heat, plotted as C/T for a series of external magnetic fields along the crystallographic c direction between 0 and 9 T. The colored background denotes for low temperatures $T < T_N$ the 3D magnetically ordered phase followed by the regime of the field-induced VC phase. The inset shows the temperature dependence of the magnetic susceptibility as measured in an external magnetic field $\mu_0 H = 0.1$ T. **b** Derivative of the magnetization with respect to the magnetic field for fields $H \parallel c$ up to 5 T taken for a series of temperatures between 3 and 15 K. For $3 \text{ K} \leq T \leq 15 \text{ K}$, (I) denotes the regime, where no magnetic or polar order is detectable, (II) the metamagnetic region with marginal macroscopic polarization, and (III) the VC phase with distinct electric polarization

average exchange of $J/k_B \approx -22 \text{ K}$.³⁹ The further increase towards low temperatures signals that the material approaches the magnetic phase transition at 2.5 K. The heat capacity, plotted as C/T (Fig. 1a) exhibits a hump-like shape close to 12 K and reveals a characteristic λ -type anomaly when crossing the AFM and FE phase boundary at 2.5 K. For increasing magnetic field, the hump slightly shifts to lower temperatures while the AFM anomaly is almost temperature independent. The low-temperature phase boundary of the AFM and FE phase agrees well with the detailed (H, T) phase diagram published in ref. ³⁷ However, there are only rare reports on the hump-like anomaly close to 12 K, weakly depending on the external field (for example, see refs. ^{39,40}). Figure 1b shows the field derivative of the magnetization up to 5 T for a series of temperatures between 3 and 15 K. Remarkably, we find a well-established metamagnetic transition close to 1.5 T, which is best developed between 3 and 8 K. We ascribe this feature partly to the crystal anisotropy. By angular-dependent electron spin-resonance experiments, the anisotropic symmetric magnetic-exchange interaction of LiCuVO_4 was determined to be of the order of 2 K, corresponding to magnetic fields of about 2 T.³⁵ Moreover, a weaker but still significant anomaly appears close to 3.5 T. Beyond 8 K, the anomalies broaden and smear out; at 15 K they finally disappear. Interestingly, all the anomalies in heat capacity and magnetization appear within the PM and paraelectric phase, well above the onset of AFM and FE order, but still below the susceptibility cusp at $\sim 25 \text{ K}$, characterizing the mean average magnetic exchange of a single spin chain. These anomalies, observed in magnetic and thermodynamic quantities, provide a first hint at the occurrence of a VC phase.

As discussed above, experimentally the most convincing proof of a VC phase is to document the appearance of spin-driven FE polarization in the absence of long-range magnetic order. Figure 2 documents the polarization P in LiCuVO_4 as function of temperature (a) and magnetic field (b) measured along the crystallographic a direction in magnetic fields applied along c . The strong increase of the polarization below $T_N \approx 2.5 \text{ K}$ (Fig. 2a) signals the onset of spin-driven ferroelectricity (c.f. saturation polarization $P_s \approx 30 \mu\text{C}/\text{m}^2$ shown in Figure S2, supplementary information). At this temperature, a 3D long-range ordered cycloidal spin-spiral evolves, propagating along b with the basal plane confined to the ab plane.^{31,36,37} According to the symmetry rules of a spin-current mechanism^{3,41} or an inverse Dzyaloshinskii–Moriya interaction,^{4,5} this spin configuration induces ferroelectricity with polarization

along a .^{36,37,42,43} However, Fig. 2a provides experimental evidence for a smaller ($\approx 0.1 P_s$) but still significant FE polarization well above T_N , a possible hallmark of a cycloidal VC phase existing beyond the 3D-ordered spiral phase.¹³ In the VC phase, the twist is ordered, but the twisting angles between neighboring spins are disordered, naturally explaining the much smaller polarization compared with the 3D-ordered spin-spiral with a coherent order of twist angles. This polarization evolves below 11 K and increases with increasing external magnetic field. However, in low magnetic fields FE polarization is absent within experimental uncertainty. To study this field effect in more detail, for temperatures between 3 and 13 K the field-dependent polarization is presented in Fig. 2b. It evidences the onset of marginal polarization at 1.5 T and a significant increase for external fields $\mu_0 H > 3 \text{ T}$. The inset in Fig. 2b shows the magnetic field dependence of the dielectric constant ϵ' at 4 K, revealing a small but well-defined peak at $\sim 3.5\text{--}4 \text{ T}$, well above T_N . It represents a characteristic feature of improper ferroelectricity, in the present case induced by a metamagnetic transition (see Fig. 1b) and signals the transition into the long-range ordered VC phase. The question remains why no FE polarization exists at low magnetic fields. Most probably, on cooling well below the susceptibility cusp where the spin spirals are already well-developed, clock- and counter clock-wise spin chiralities are statistically distributed. This is certainly true for neighboring spin chains, which are only weakly coupled, but could also be valid for spin fragments within one chain. We assign this phase with fluctuating spin chiralities as vector-chiral spin liquid (VCL). Here, it is important to note that, without applying an electric field while cooling the system below 12 K, no chirality-induced FE polarisation can be detected (see supplementary information, inset of Figure S2b: pyrocurrent measurement with and without electric field cooling in an applied magnetic field of $H_c = 7 \text{ T}$). However, our experiments document that an external magnetic field perpendicular to the basal plane of the spin rotation is needed to switch all chiralities into one direction, leading to macroscopic FE polarization. This is established at fields close to 4 T by the strong increase of FE polarization and by the peak-like anomaly in the dielectric constant (see Fig. 2b). This finding is unexpected and will be outlined in more detail below.

In addition, for $P \parallel a$ in applied magnetic fields along the b -direction (see supplementary information, Figure S2a) no FE signature is detected above T_N . This finding excludes a FE polarisation along a . The case of $P \parallel a$ and $H \parallel a$ (not shown) would

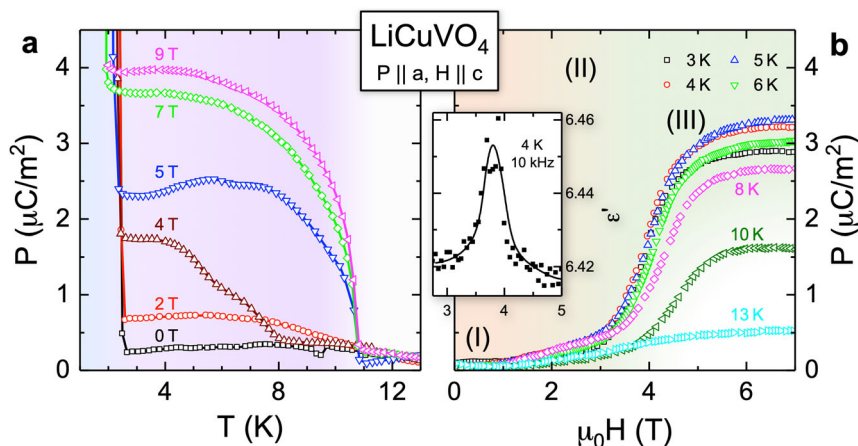


Fig. 2 Polarization of LiCuVO_4 in the region of the VC phase. **a** Temperature dependence of the electric polarization along the crystallographic **a** direction, $P||\mathbf{a}$, for a series of magnetic fields $\mu_0 H$, between 0 and 9 T with $H||\mathbf{c}$. The colored background denotes for low temperatures $T < T_N$ the 3D magnetically ordered phase followed by the regime of the field-induced VC phase. **b** Field dependence of the polarization $P||\mathbf{a}$ for a series of temperatures between 3 and 13 K. The inset shows the magnetic field dependence of the dielectric constant measured at 4 K, well above T_N . (I) denotes the regime, where neither long-range magnetic nor polar order is detectable (VCL), (II) a transition region indicated by a metamagnetic anomaly with marginal polarization only, and (III) the PM VC phase with distinct FE polarization

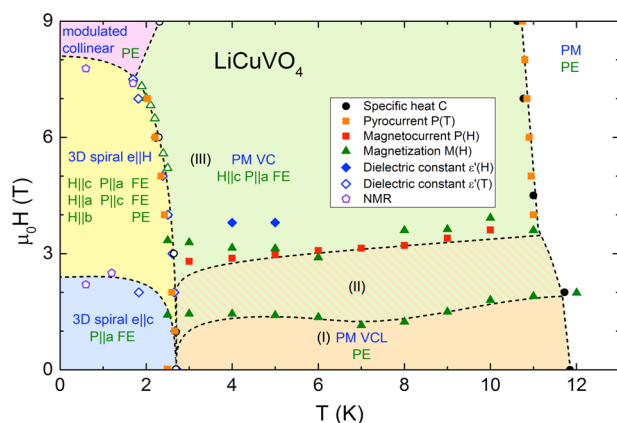


Fig. 3 (H, T) phase diagram of LiCuVO_4 . Results from the present work (closed symbols) and from ref. ³⁷ (open symbols, i.e., results from specific heat, magnetization, dielectric constant and NMR measurements) were used. Anomalies observed by different measuring techniques are characterized by different symbols (see figure legend). Magnetic (blue lettering) and electric phases (green lettering) are indicated in the different regimes. The VC phase is indicated by the light-green area (III). This phase evolves at 3 T and extends at least up to 9 T. Its upper limit could not be identified in the present work. At low external fields up to 1.5 T a VCL phase (I) with fluctuating chiralities is established. The intermediate phase (II) (dashed area) could not be uniquely identified

imply a possible tilting of the VC into an unfavoured direction of the spin plane, which already reduces the net polarisation in the 3D-ordered phase by a factor of ten.^{36,37,43} A possible pyro- or magnetocurrent signal is below the resolution limit, impeding the analysis of a switched polarisation⁴² within the VC phase, which requires further investigations.

DISCUSSION

These experiments—together with results obtained earlier³⁷—allow for the construction of a detailed (H, T) phase diagram of LiCuVO_4 including the 3D spin-spiral phases and the advocated VC phase extending to higher temperatures well into the PM regime (Fig. 3). Below 2.5 K, an AFM regime with long-range magnetic order and concomitant spin-driven ferroelectricity shows up. As

discussed in detail in ref. ³⁷ in the long-range magnetically ordered phase and at zero external magnetic field, the spiral axis **e** is oriented parallel to the crystallographic **c** direction and the spiral propagates along **b**, resulting in a polarization along **a**. Increasing magnetic fields along **c** leave the spin-spiral axis and, hence, the polarization unchanged. At 8 T the system undergoes a transition into a modulated collinear structure with zero polarization.³⁷ In the present work, we investigated the temperature and field regime up to 15 K and 9 T, identifying an extended region with finite FE polarization, above 3 T and up to temperatures of 11 K (Fig. 2). From these experiments, we conclude that the low-field regime is characterized by zero polarization, whereas for higher fields, $\mu_0 H > 3$ T, a significant polarization evolves.

The natural explanation for the occurrence of this polarization is the existence of a PM VC phase in LiCuVO_4 , developing at temperatures well above the onset of long-range magnetic order. This VC phase is characterized by long-range order of the spin chirality, however with statistical distribution of twist angles. When entering the low-temperature spin-spiral phase coherent order of the twist angles is established, providing long-range ordered spin correlations. Zero polarization in low fields probably results from fluctuating spin chiralities leading to a VCL phase. Between 1.5 T and 3 T we find an intermediate phase with marginal FE polarization. It could result from a distinct magnetic anisotropy.³⁵ However, it also could indicate that the phase diagram in LiCuVO_4 is even more complex with further chiral, multipolar, or nematic-type phases as have been theoretically predicted.^{18,19} Even domain-like objects of spin spirals with different rotation sense may play a role, leading to an extended temperature range for which vector chirality is stabilized.^{44,45}

It should be noted that in the specific heat, the transition into the vector-chiral phase only shows up as a broad hump (Fig. 1a), while at the formation of long-range spin order at T_N , a strong and sharp heat-capacity anomaly shows up. However, at the transition into the proposed vector-chiral phase at ~ 12 K, only a single degree of freedom, the chirality, becomes ordered. It seems natural that this should lead to a smaller entropy change and, thus, a much weaker anomaly as indeed found in our experiments. Notably, the maximum polarization found in the vector-chiral phase also is significantly smaller than in the fully ordered phase. Obviously, more work is necessary to clarify this issue.

As an alternative explanation for the observed polarization occurring at 12 K, one could consider pre-transitional effects, such as the phase separation into spiral and PM phases induced by

disorder, i.e., the polarization could be induced by short-range spiral order. However, in all previous publications on LiCuVO_4 , there were no reports of any significant enhancement of the long-range magnetic ordering temperature. Even for strongly heterogeneous samples, an enhancement of the ordering temperature by a factor of five seems hard to imagine as, in this case, the inter-chain coupling, leading to the long-range order, has to be considerably enhanced. Moreover, we want to remark that within a phase-separation scenario, it would be hard to explain the absence of any polar order in low magnetic fields. Below T_N , spin-driven polar order appears even in zero magnetic field, which should also be the case for the enhanced magnetic transition temperature in the phase-separated regions.

From our point of view, a more likely explanation of the electrical polarization properties at temperatures $2.5 \text{ K} < T < 12 \text{ K}$ is based on the suggestion, that a long-range three-dimensional VC structure is established within all phases I, II, and III of the H - T phase diagram presented in Fig. 3. However, in this case it has to be assumed that the spiral plane reorients when passing the AFM phase boundary. In the PM phase and in the range of small fields (phase I), the vector chirality of the spin plane is oriented perpendicular to the crystallographic c direction, with zero electrical polarization along \mathbf{a} . Note that there are two equivalent magnetic domains with opposite chirality. At magnetic fields of 4 T with $H \parallel c$, the chirality vector for both domains flips to the $\pm c$ direction with random sign. Hence, the FE polarizations of both domains compensate each other. To establishing macroscopic FE polarization along \mathbf{a} (phase III), the magnetic domain with preferred chirality must be pre-selected by the applied electric field on cooling. As explained above, FE polarization above T_N was only detected after cooling the sample in electric fields. At the same time, this pre-selection is most likely responsible for the slightly increasing polarization of phase II. The suggested spin-plane reorientation at T_N could be driven by competing anisotropic magnetic exchange in the VC phase. In zero external fields, the orientation of the spin plane of the VC phase is assumed to differ from the orientation of the basal plane of the spiral structure observed at $T < T_N$. The possible change of the anisotropy in LiCuVO_4 at T_N from easy-plane in the 3D AFM phase to easy-axis in the PM phase is supported by PM-resonance experiments.³⁵

In summary, by measuring the polarization and dielectric constant in LiCuVO_4 as function of temperature and magnetic field, we provide experimental evidence of FE polarization in its PM phase, well above the well-known multiferroic phases. The existence of a VC phase with long-range ordered chiralities as a precursor of spin order is the most plausible explanation. Hence, our results provide the long-sought experimental proof of the theoretically predicted existence of a VC phase, in close analogy to cholesteric liquid crystals¹² via polarization measurements. We confirm the expectation that spin chirality without long-range spin order occurs prior to 3D spin-spiral order.¹³ We demonstrate that the spin twist in a VC phase induces ferroelectricity, just as in conventional spin-spiral magnets, however, with much lower polarisation. It would be highly interesting to perform neutron-scattering experiments on LiCuVO_4 in applied magnetic fields $H \parallel c$, specifically focusing on the occurrence of this VC state.

METHODS

LiCuVO_4 single crystals have been prepared as described in ref. ⁴⁶ They crystallize in the space group $Imma$ and undergo a transition into an AFM phase at $\sim 2.5 \text{ K}$. The crystals have typical sizes of $3 \times 3 \times 1 \text{ mm}^3$ and were oriented by Laue diffraction techniques. The single crystals used in the course of this work were characterized by magnetic susceptibility and magnetic resonance techniques,^{35,47} as well as by dielectric techniques.^{37,42} For detailed magnetization and heat-capacity experiments, we utilized a Quantum Design Magnetic Property Measurement System with

external magnetic fields up to 5 T and a Quantum Design Physical Property Measurement System (PPMS) using magnetic fields up to 9 T. The dielectric measurements were performed with electric fields applied along the crystallographic directions, with silver-paint contacts either in sandwich geometry or in a cap-like fashion, covering the opposite ends of the sample. The complex dielectric constants were measured for frequencies between 100 Hz and 10 kHz employing an Andeen-Hagerling AH2700A high-precision capacitance bridge. For measurements between 1.8 and 300 K and in external magnetic fields up to 9 T, a Quantum Design PPMS was used. To probe FE polarization, we measured both, the pyrocurrent at fixed magnetic field and the magnetocurrent at fixed temperature using a Keithley 6517A electrometer. To align the FE domains on cooling, electric poling fields of the order 1 kV/cm were applied.

DATA AVAILABILITY

Measurement data supporting the findings of this study are available from the corresponding author S.K. upon reasonable request.

ACKNOWLEDGEMENTS

A.R., P.L., H.K., A.L., and S.K. acknowledge funding from the Deutsche Forschungsgemeinschaft (DFG) via the Transregional Collaborative Research Center TRR80 (Augsburg, Munich) and the BMBF via ENREKON 03EK3015. L.S. acknowledges funding from the Russian Science Foundation Grant No.17-02-01505. We thank Manfred Fiebig for very useful discussions.

AUTHOR CONTRIBUTIONS

A.R. conducted the magnetic, specific heat, and dielectric measurements under the supervision of S.K. The specific heat data were analyzed by H.K. and S.W. A.P. grew the crystal. P.L., H.K., L.S., A.L., and S.K. analyzed the experimental data. S.K. initiated and coordinated this project and A.L. wrote the manuscript, supported by P.L., H.K., and S.K. All authors discussed the results and contributed to the final version of the manuscript.

ADDITIONAL INFORMATION

Supplementary information accompanies the paper on the *npj Quantum Materials* website (<https://doi.org/10.1038/s41535-019-0163-2>).

Competing interests: The authors declare no competing interests.

Publisher's note: Springer Nature remains neutral with regard to jurisdictional claims in published maps and institutional affiliations.

REFERENCES

- Mostovoy, M. Multiferroic propellers. *Physics* **5**, 16 (2012).
- Kimura, T. et al. Magnetic control of ferroelectric polarization. *Nature* **42**, 55 (2003).
- Katsura, H., Nagaosa, N. & Balatsky, A. V. Spin current and magnetoelectric effect in noncollinear magnets. *Phys. Rev. Lett.* **95**, 057205 (2005).
- Mostovoy, M. Ferroelectricity in spiral magnets. *Phys. Rev. Lett.* **96**, 067601 (2006).
- Sergienko, I. A. & Dagotto, E. Role of the Dzyaloshinskii-Moriya interaction in multiferroic perovskites. *Phys. Rev. B* **73**, 094434 (2006).
- Fiebig, M. Revival of the magnetoelectric effect. *J. Phys. D.* **38**, R123 (2005).
- Cheong, S.-W. & Mostovoy, M. Multiferroics: a magnetic twist for ferroelectricity. *Nat. Mater.* **6**, 13 (2007).
- Ramesh, R. & Spaldin, N. A. Multiferroics: progress and prospects in thin films. *Nat. Mater.* **6**, 21 (2007).
- Starykh, O. A. Unusual ordered phases of highly frustrated magnets: a review. *Rep. Prog. Phys.* **78**, 052502 (2015).
- Villain, J. Two-level systems in a spin-glass model. I. General formalism and two-dimensional model. *J. Phys. C: Sol. Stat. Phys.* **10**, 4793 (1977).
- Chubukov, A. V. Chiral, nematic, and dimer states in quantum spin chains. *Phys. Rev. B* **44**, 4693 (1991).
- Villain, J. Proceedings of the 13th IUPAP Conference on Statistical Physics. *Ann. Isr. Phys. Soc.* **2**, 565 (1978).
- Onoda, S. & Nagaosa, N. Chiral spin pairing in helical magnets. *Phys. Rev. Lett.* **99**, 027206 (2007).
- Hikihara, T., Kaburagi, M. & Kawamura, H. Ground-state phase diagrams of frustrated spin-5 XXZ chains: chiral ordered phases. *Phys. Rev. B* **63**, 174430 (2001).

15. Kolezhuk, A. & Vekua, T. Field-induced chiral phase in isotropic frustrated spin chains. *Phys. Rev. B* **72**, 094424 (2005).
16. Heidrich-Meisner, F., Honecker, A. & Vekua, T. Frustrated ferromagnetic spin-1/2 chain in a magnetic field: the phase diagram and thermodynamic properties. *Phys. Rev. B* **74**, 020403(R) (2006).
17. McCulloch, I. P. et al. Vector chiral order in frustrated spin chains. *Phys. Rev. B* **77**, 094404 (2008).
18. Hikihara, T., Kecke, L., Momoi, T. & Furusaki, A. Vector chiral and multipolar orders in the spin-1/2 frustrated ferromagnetic chain in magnetic field. *Phys. Rev. B* **78**, 144404 (2008).
19. Sudan, J., Lüscher, A. & Läuchli, A. M. Emergent multipolar spin correlations in a fluctuating spiral: the frustrated ferromagnetic spin-1/2 Heisenberg chain in a magnetic field. *Phys. Rev. B* **80**, 140402(R) (2009).
20. Furukawa, S., Sato, M. & Onoda, S. Chiral order and electromagnetic dynamics in one-dimensional multiferroic cuprates. *Phys. Rev. Lett.* **105**, 257205 (2010).
21. Sato, M., Hikihara, T. & Momoi, T. Field and temperature dependence of NMR relaxation rate in the magnetic quadrupolar liquid phase of spin-1/2 frustrated ferromagnetic chains. *Phys. Rev. B* **83**, 064405 (2011).
22. Guo, X., Li, Y. & Jia, C. Vector-spin-chirality bound state driven by the inverse Dzyalohinskii-Moriya mechanism. *New. J. Phys.* **20**, 053032 (2018).
23. Parvej, A. & Kumar, M. Degeneracies and exotic phases in an isotropic frustrated spin-1/2 chain. *J. Magn. Magn. Mater.* **401**, 96 (2016).
24. Cinti, F. et al. Two-step magnetic ordering in quasi-one-dimensional helimagnets: possible experimental validation of villain's conjecture about a chiral spin liquid phase. *Phys. Rev. Lett.* **100**, 057203 (2008).
25. Schenk, H., Pokrovsky, V. L. & Nattermann, T. Vector chiral phases in the frustrated 2D XY model and quantum spin chains. *Phys. Rev. Lett.* **112**, 157201 (2014).
26. Svistov, L. E. et al. New high magnetic field phase of the frustrated $S=1/2$ chain compound LiCuVO_4 . *JETP Lett.* **93**, 21 (2011).
27. Mourigal, M. et al. Evidence of a bond-nematic phase in LiCuVO_4 . *Phys. Rev. Lett.* **109**, 027203 (2012).
28. Nawa, K., Takigawa, M., Yoshida, M. & Yoshimura, K. Anisotropic spin fluctuations in the quasi one-dimensional frustrated magnet LiCuVO_4 . *J. Phys. Soc. Jpn.* **82**, 094709 (2013).
29. Büttgen, N. et al. Search for a spin-nematic phase in the quasi-one-dimensional frustrated magnet LiCuVO_4 . *Phys. Rev. B* **90**, 134401 (2014).
30. Orlova, A. et al. Nuclear magnetic resonance signature of the spin-nematic phase in LiCuVO_4 at high magnetic fields. *Phys. Rev. Lett.* **118**, 247201 (2017).
31. Enderle, M. et al. Quantum helimagnetism of the frustrated spin-1/2 chain LiCuVO_4 . *Europhys. Lett.* **70**, 237 (2005).
32. Nishimoto, S. et al. The strength of frustration and quantum fluctuations in LiV-CuO_4 . *Europhys. Lett.* **98**, 37007 (2012).
33. Koo, H.-J., Lee, Ch, Whangbo, M.-H., McIntyre, G. J. & Kremer, R. K. On the nature of the spin frustration in the CuO_2 ribbon chains of LiCuVO_4 : crystal structure determination at 1.6 K, magnetic susceptibility analysis, and density functional evaluation of the spin exchange constants. *Inorg. Chem.* **50**, 3582 (2011).
34. Vasil'ev, A. N. et al. Magnetic and resonant properties of quasi-one-dimensional antiferromagnet LiCuVO_4 . *Phys. Rev. B* **64**, 024419 (2001).
35. Krug von Nidda, H.-A. et al. Anisotropic exchange in LiCuVO_4 probed by ESR. *Phys. Rev. B* **65**, 134445 (2002).
36. Naito, Y., Sato, K., Yasui, Y., Kobayashi, Y. & Sato, M. Ferroelectric transition induced by the incommensurate magnetic ordering in LiCuVO_4 . *J. Phys. Soc. Jpn.* **76**, 023708 (2007).
37. Schrettle, F. et al. Switching the ferroelectric polarization by external magnetic fields in the spin-1/2 chain cuprate LiCuVO_4 . *Phys. Rev. B* **77**, 144101 (2008).
38. Johnston, D. C. et al. Thermodynamics of spin $S=1/2$ antiferromagnetic uniform and alternating-exchange Heisenberg chains. *Phys. Rev. B* **61**, 9558 (2000).
39. Yamaguchi, M., Furuta, T. & Ishikawa, M. Calorimetric study of several cuprates with restricted dimensionality. *J. Phys. Soc. Jpn.* **65**, 2998 (1996).
40. Prozorova, L. A. et al. Magnetic field driven 2D-3D crossover in the $S=1/2$ frustrated chain magnet LiCuVO_4 . *Phys. Rev. B* **91**, 174410 (2015).
41. Mourigal, M., Enderle, M., Kremer, R. K., Law, J. M. & Fåk, B. Ferroelectricity from spin supercurrents in LiCuVO_4 . *Phys. Rev. B* **83**, 100409(R) (2011).
42. Ruff, A., Krohns, S., Lunkenheimer, P., Prokofiev, A. & Loidl, A. Dielectric properties and electrical switching behaviour of the spin-driven multiferroic LiCuVO_4 . *J. Phys: Condens. Matter* **26**, 485901 (2014).
43. Yasui, Y. et al. Relationship between magnetic structure and ferroelectricity of LiVCuO_4 . *J. Phys. Soc. Jpn.* **77**, 023712 (2008).
44. Shang, T. et al. Design of magnetic spirals in layered perovskites: extending the stability range far beyond room temperature. *Sci. Adv.* **4**, eaau6386 (2018).
45. Scaramucci, A. et al. Multiferroic magnetic spirals induced by random magnetic exchanges. *Phys. Rev. X* **8**, 011005 (2018).
46. Prokofiev, A. V., Wichert, D. & Aßmus, W. Crystal growth of the quasi-one dimensional spin-magnet LiCuVO_4 . *J. Cryst. Growth* **220**, 345 (2000).
47. Büttgen, N. et al. Spin-modulated quasi-one-dimensional antiferromagnet LiCuVO_4 . *Phys. Rev. B* **76**, 014440 (2007).



Open Access This article is licensed under a Creative Commons Attribution 4.0 International License, which permits use, sharing, adaptation, distribution and reproduction in any medium or format, as long as you give appropriate credit to the original author(s) and the source, provide a link to the Creative Commons license, and indicate if changes were made. The images or other third party material in this article are included in the article's Creative Commons license, unless indicated otherwise in a credit line to the material. If material is not included in the article's Creative Commons license and your intended use is not permitted by statutory regulation or exceeds the permitted use, you will need to obtain permission directly from the copyright holder. To view a copy of this license, visit <http://creativecommons.org/licenses/by/4.0/>.

© The Author(s) 2019